Selective, competitive and mechanism-based inhibitors of human cytochrome P450 2J2.

Pierre Lafite, Sylvie Dijols, Darryl C Zeldin, Patrick M Dansette, Daniel Mansuy

Running title : Inhibitors of CYP2J2

SELECTIVE, COMPETITIVE AND MECHANISM-BASED INHIBITORS OF HUMAN CYTOCHROME P450 2J2

Pierre LAFITE[a], Sylvie DIJOLS[a], Darryl C. ZELDIN[b], Patrick M. DANSETTE[a] and Daniel MANSUY[a*]

[a] Laboratoire de Chimie et Biochimie Pharmacologiques et Toxicologiques - UMR 8601 Université Paris Descartes, CNRS, 45 Rue des Saints-Pères, 75270 Paris Cedex 06, France

[b]NIEHS, National Institutes of Health, Research Triangle Park, North Carolina 27709, USA

*To whom correspondence should be addressed

Tel.: 33 (0)1 42 86 40 62; fax: 33 (0)1 42 86 83 87

E-mail: daniel.mansuy@univ-paris5.fr

ABSTRACT

Twenty five derivatives of the drugs terfenadine and ebastine have been designed, synthesized, and evaluated as inhibitors of recombinant human CYP2J2. Compound **14**, that involves an imidazole substituent, is a good non competitive inhibitor of CYP2J2 (IC_{50} = 400 nM). It is not selective towards CYP2J2 as it also efficiently inhibits the other main vascular CYPs, such as CYP2B6, 2C8, 2C9 and 3A4; however, it could be an interesting tool to inhibit all these vascular CYPs. Compounds **4**, **5** and **13** that involve a propyl, allyl and benzo-1,3-dioxole terminal groups, respectively, are selective CYP2J2 inhibitors. Compound **4** is a high-affinity, competitive inhibitor and alternative substrate of CYP2J2 (K_i = 160 ± 50 nM). Compound **5** and **13** are efficient mechanism-based inhibitors of CYP2J2 (k_{inact}/K_I values ~3000 $L.mol^{-1}.s^{-1}$). Inactivation of CYP2J2 by **13** is due to the formation of a stable iron-carbene bond which occurs upon CYP2J2-catalyzed oxidation of **13** with a partition ratio of 18 ± 3. These new selective inhibitors should be interesting tools to study the biological roles of CYP2J2.

KEYWORDS

Ebastine; terfenadine; drug metabolism; arachidonic acid epoxidation; vascular P450s; benzo-1,3-dioxole; hydroxylation; monooxygenases; hemeproteins.

ABBREVIATIONS

CYP or P450: cytochrome P450; DMF: N,N-dimethylformamide; DMSO: dimethylsulfoxide; EDTA: ethylenediaminetetraacetic acid; EET: epoxyeicosatrienoic acid; ESI: electrospray ionization; GSH: glutathione, reduced form; HEPES: 4-(2-hydroxyethyl)-1-piperazineethanesulfonic acid; HPLC: high performance liquid chromatography; MS: mass spectrometry; MS^2: tandem mass spectrometry; THF: tetrahydrofuran; TLC: thin layer chromatography; Tris: 2-amino-2-(hydroxymethyl)-1,3-propanediol; UV: ultraviolet.

INTRODUCTION

Cytochromes P450 (CYPs) constitute a superfamily of hemoproteins that play key roles in the metabolism of a large variety of xenobiotics and endogenous compounds [1]. In the human genome, 57 genes have been found to code for CYPs [2]. The main CYPs implicated in drug metabolism, such as CYP3A4, CYP2C9 or CYP2D6, and those responsible for the biosynthesis of steroid hormones have been extensively studied, and several x-ray structures of human CYPs have been recently published [3-10]. Much less is known about more recently discovered human CYPs such as CYP2J2 [2, 11, 12]. This cytochrome seems to be primarily expressed in heart [11]; it has also been found in kidney, liver, lung and the gastrointestinal tract [11-14]. CYP2J2 has been found to catalyze the epoxidation of arachidonic acid to four cis-epoxyeicosatrienoic acids (EETs), with regio- and stereo- selectivities that match those of the EETs isolated from heart tissue [11]. Some EETs-derived metabolites play important roles in the regulation of vascular tone [15, 16]. Moreover, it has been shown that CYP2J2-derived metabolites are involved in the recovery of heart function following ischemia in mice[17], that the risk of coronary artery disease is associated with polymorphisms in CYP2J2 gene in humans [18], and that CYP2J2-derived products are involved in cardiac electrophysiology [19, 20]. EETs and EETs-derived metabolites are also involved in a host of processes related to cancer cell behavior, angiogenesis and tumor pathogenesis [21, 22]. Very recent data suggest that CYP2J2 promotes the neoplastic phenotype of carcinoma cells and may represent a novel biomarker and potential target for therapy of human cancers [23]. Besides these possible roles in the metabolism of endogenous compounds, CYP2J2 could be implied in the metabolism of some drugs, especially at the intestinal level. Thus, CYP2J2 has been shown to contribute to the metabolism of three drugs, ebastine [24, 25], astemizole [26] and terfenadine [27].

Little data are presently available on the active site topology and substrate specificity of CYP2J2 [2]. Quite recently, preliminary results have shown that it was possible to obtain high-affinity inhibitors for CYP2J2, by chemical modification of terfenadone [28], that is an isomer of ebastine and a derivative of the drug terfenadine (see Figure 1 and Table 1). This article describes the design, synthesis, and evaluation as CYP2J2 inhibitors of 25 derivatives of terfenadone and ebastine. It also reports the compared effects of these compounds towards the other main CYPs that are present in the vascular system, such as CYP2B6, 2C8, 2C9 and 3A4. Finally, it describes a detailed study of the mechanism of inhibition of CYP2J2 by some of these compounds and reveals a high-affinity and selective, competitive inhibitor of CYP2J2, and two selective, mechanism-based inhibitors of CYP2J2.

MATERIALS AND METHODS

Commercial chemicals.

All chemicals used in this study were of the highest purity available. Organic and HPLC solvents were purchased from SDS (Peypin, France); ebastine was provided by Almirall (Paris, France). $NADP^+$, glucose 6-phosphate and glucose 6-phosphate dehydrogenase were purchased from Boehringer-Mannheim (Mannheim, Germany). Paclitaxel, amodiaquine, reduced glutathione (GSH), 7-benzyloxyresorufin, resorufin, diclofenac, testosterone, ticlopidine, sulfaphenazole and ketoconazole were obtained from Sigma chemicals (Lyon, France). 3',4'-Dihydroxypropiophenone and 3,4-(methylenedioxy)propiophenone were purchased from Alfa Aesar (Strasbourg, France). Montelukast was obtained from Sequoia Research (Oxford, UK).

Physical measurements.

UV-visible spectra were recorded at room temperature using an Uvikon 941 spectrophotometer. ^{1}H NMR spectra were recorded at 27 °C on a Bruker ARX-250 instrument; chemical shifts are reported downfield from $(CH_3)_4Si$ and coupling constants are in Hz. The abbreviations s, d, t, q, m, bs, dd, dt, td and tt are used for singlet, doublet, triplet, quadruplet, massif, broad singlet, doublet of doublets, doublet of triplets, triplet of doublets and triplet of triplets, respectively. Mass spectra (MS) were performed using a LCQ Advantage-ion trap mass spectrometer (Thermo Finnigan, Les Ulis, France). MS ionization was carried out using an electrospray ionization (ESI) source in positive mode, with a capillary temperature of 275 °C, a capillary voltage of 21 V and a spray voltage of 5 kV. This ionization gave the molecular ion ($M+H^+$) indicated for each compound. The mentioned fragments were obtained from tandem mass spectrometry (MS^2) that was performed with activated broadband and a fragmentation power set to 40-50 %, depending on the substrate. Compound **11** contains one bromine atom, and all peaks corresponding to the molecular ion or fragments involving a Br atom exhibited the isotope cluster expected for the presence of one Br atom (with a M:M+2 ratio of 51:49).

Synthesis of ebastine and terfenadone derivatives.

All compounds were characterized by ^{1}H NMR spectroscopy in $CDCl_3$ and ESI-ion trap MS^2 in positive mode. ^{1}H NMR spectroscopy analysis in the presence of an internal standard showed that all these compounds were more than 95 % pure. Most compounds were synthesized according to the scheme indicated on Fig. 2. This was the case of compounds **1**, **3**, **4**, **6-9**, **11-13**, **15** and **19-21**. Compounds **5** and **14** were prepared from **11**. Compound **17** was synthesized by a very similar protocol using 4-(4-propylphenyl)butylmethane sulfonate as an intermediate. Compounds **2**, **10**, **16**, and **25** were a gift from Dr. Didier Buisson (UMR 8601, Paris); their syntheses will be described elsewhere (El Ouarradi *et al.*, in preparation).

Finally, compounds **22**, **23**, and **24** were obtained from dehydration of **1**, **15**, and terfenadine, respectively. Compounds **1**, **11**, **20**, **22** and **24** were reported in a patent [29]; however their ^{1}H NMR and mass spectrum characteristics were not described. The main ^{1}H NMR and MS characteristics of compounds **1**, **3**, **4**, **6**, **9**, **11-13**, **15**, **17**, **5**, **14**, **7**, **8**, **19**, **18**, and **21-24** (in the order of appeareance in following paragraphs *a)* to *h)*) as well as those of some of their precursors are given in Supplementary Materials.

a) Synthesis of the intermediates (see Fig. 2).

4-(diphenylmethoxy)piperidine [30] and 1,1-difluoro-2-phenylethane [31] were prepared as described previously.

Typical procedure for the synthesis of the intermediate alkylchlorides by Friedel-Crafts acylations. To a solution of aromatic starting compound C_6H_5-**R** (see Fig. 2) (15 mmol) and 4-chlorobutanoyl chloride (15 mmol) in dry CH_2Cl_2, $AlCl_3$ or $SnCl_4$ (20 mmol) was progresssively added at room temperature under argon. After stirring at room temperature for 2-18 h then at 40°C for 2-7 h, the mixture was poured into ice water and stirred overnight. The organic phase was separated and the aqueous phase was extracted with CH_2Cl_2. The combined extract was dried ($MgSO_4$) and the solvent evaporated. Compounds were purified by column chromatography (SiO_2) (cyclohexane/ethyl acetate 90/10). The obtained alkylchlorides were characterized by ^{1}H NMR spectroscopy and used as such for the following reactions.

Synthesis of 4-(4-propylphenyl)butylmethanesulfonate. 4-(4-Propylphenyl)butanoic acid was prepared as described previously [32, 33]. A solution of this carboxylic acid (1.03 g, 5 mmol) in THF (10 mL) was slowly added to a suspension of $NaBH_4$ (227 mg, 6 mmol) in THF (10 mL) at room temperature (10 min). The mixture was stirred until the end of gas emission. Iodine (635 mg, 2.5 mmol) in THF (10 mL) was then added slowly (10 min) at room

temperature. The medium was further stirred for 1h. Dilute HCl (7 mL, 1N) was added carefully and the mixture extracted with ether. The combined ether extracts were washed with 1M NaOH and brine, and dried over $MgSO_4$. Evaporation of the organic layer gave 4-(4-propylphenyl)butan-1-ol which was purified by column chromatography on SiO_2 (CH_2Cl_2 then +10% ether), and was obtained as a pale yellow oil in a 61 % yield. ^{1}H NMR ($CDCl_3$): δ 0.92 (3H, t, *J = 7.3 Hz*), 1.19 (1H, bs), 1.65 (6H, m), 2.56 (4H, m), 3.65 (2H, m), 7.07 (4H, s). Methanesulfonyl chloride (326 µL, 4.22 mmol) was then added to a stirred solution of this alcohol (405 mg, 2.11 mmol) in dry CH_2Cl_2 (6.5 mL) containing pyridine (1.48 mL) at 0°C. This solution was stirred under an argon atmosphere for 20 h at room temperature, diluted with CH_2Cl_2, washed with aqueous sulfuric acid (1%, 2 x 50 mL), saturated aqueous $NaHCO_3$ (50 mL), and brine, and reextracted with CH_2Cl_2. The combined organic phase was dried ($MgSO_4$), and the solvent was removed under vacuum to afford a colourless oil (100% yield). ^{1}H NMR ($CDCl_3$): δ 0.92 (3H, t, *J = 7.6 Hz*), 1.61 (2H, m), 1.65 (4H, m), 2.53 (2H, t, *J = 7.6 Hz*), 2.61 (2H, m), 2.96 (3H, s), 4.21 (2H, t, *J = 5.8 Hz*), 7.07 (4H, s).

b) General procedure for N-alkylation of α,α-diphenyl-4-piperidinomethanol (terfenadone derivatives) or 4-(diphenylmethoxy)piperidine (ebastine derivatives) [34], used for the synthesis of **1**, **3**, **4**, **6**, **7**, **9**, **11**-**13**, **15**, and **17**.

The piperidine derivative (1 eq.), anhydrous K_2CO_3 (2 eq.) and KI (0.2 eq.) were added to a solution of 4-chlorobutan-1-one-derived compounds (1 eq.) in dry DMF. The resulting mixture was refluxed under argon for 24 h. After cooling, the solvent was removed under vacuum to give a residue that was dissolved in CH_2Cl_2, washed with water, and dried over $MgSO_4$. After evaporation of the solvent, products were purified by column chromatography on SiO_2 (CH_2Cl_2 then 10% MeOH), and by dissolution in ether to filter the insoluble impurities.

c) Synthesis of 1-(4-allylphenyl)-4-(4-(hydroxydiphenylmethyl)piperidin-1-yl)butan-1-one, **5**.

Coupling of **11** (620 mg, 1.26 mmol) with allyltributyltin (0.5 mL) in DMF (13 mL) was performed in the presence of tetrakis(triphenylphosphine)palladium(0) (90 mg) under argon, 30 min at room temperature then 6 h at 110°C. Purification by column chromatography (SiO_2 CH_2Cl_2 - MeOH 95:5) led to compound **5** as a white powder in 45% yield.

d) Preparation of 1-(4-N-imidazolylphenyl)-4-(4-(hydroxydiphenylmethyl)piperidin-1-yl)butan-1-one, **14**.

Coupling of **11** (0.13 mmol) with imidazole (0.16 mmol) was performed in the presence of CuI (0.013 mmol), proline (0.13 mmol) and K_2CO_3 (0.26 mmol) [35]. The reaction was performed under argon at 95°C during 40 h. After ethyl acetate extraction and drying on anhydrous $MgSO_4$, **14** was purified on SiO_2 (CH_2Cl_2/MeOH 90:10) and led to a brown oil (54 % yield)

e) Preparation of 4-(4-(hydroxydiphenylmethyl)piperidin-1-yl)-1-(4-(2-hydroxyethyl)phenyl)butan-1-one, **7**, *4-(4-(hydroxydiphenylmethyl)piperidin-1-yl)-1-(4-(3-hydroxypropyl)phenyl)butan-1-one,* **8**, *and 4-(4-(diphenylmethoxy)piperidin-1-yl)-1-(4-(2-hydroxyethyl)phenyl)butan-1-one,* **19**, *from their acetate precursors.*

The acetate precursor (1 mmol) was heated under reflux in 5 mL EtOH with 70 mg NaOH (1.75 mmol) for 2.5 h. After evaporation of EtOH, the residue was diluted with water and extracted with CH_2Cl_2. The organic phase was dried over $MgSO_4$. After evaporation of the solvent, compounds **7**, **8** and **19** were purified by column chromatography (SiO_2, CH_2Cl_2 - EtOH 90:10) and by dissolution in ether to filter insoluble impurities.

f) Synthesis of 4-(4-(diphenylmethoxy)piperidin-1-yl)-1-(4-(2-tertiobutyl)phenyl)butan-1-ol, **18**, *from reduction of ebastine.*

A suspension of $NaBH_4$ (64,4 mg, 1.7 mmol) in MeOH (4 mL) was slowly added to a solution of ebastine (200 mg, 0.4 mmol) in distilled THF (8 mL) at 0°C. After 7h of stirring, HCl (1 mL, 1 M) was added to hydrolyze residual $NaBH_4$ and the mixture was extracted with ethyl acetate. The combined extract was washed with brine and dried over Na_2SO_4. After filtration, **18** was purified by column chromatography on SiO_2 (CH_2Cl_2 then 5 % MeOH) and was obtained as white powder in 81 % yield.

g) Synthesis of (4-[4-(diphenylmethoxy)piperidin-1-yl]-1-(4-vinylphenyl)butan-1-one, **20**, *and 4-[4-(diphenylmethoxy)piperidin-1-yl]-1-[4-(2-thiomethoxy)ethylphenyl]butan-1-one,* **21**, *from* **19**.

Compound **19** (100mg, 0.22mmol) in the presence of ethylamine (30µL, 0.21 mmol) was cooled to 0°C in CH_2Cl_2 (2mL). Methanesulfonyl chloride (20 µL, 0.26 mmol) was added and the reaction mixture was kept at 0°C for 2h. After evaporation, 2-(4-{4-[4-(diphenylmethoxy)piperidin-1-yl]-1-oxobutyl}phenyl)ethyl methanesulfonate was purified by column chromatography (SiO_2, CH_2Cl_2 then 7 % EtOH). Then, dissolution in ether to filter insoluble impurities gave the desired product (110mg, 0.21 mmol, 95 % yield). ^{1}H NMR ($CDCl_3$): δ 1.66 (2H, m), 1.91 (4H, m), 2.12 (4H, m), 2.37 (2H, t, *J = 7.1 Hz*), 2.86 (3H, s), 2.95 (2H, t, *J = 7.1 Hz*), 3.09 (2H, t, *J = 6.7 Hz*), 3.40 (1H, m), 4.42 (2H, t, *J = 6.7 Hz*), 5.48 (1H, s), 7.17-7.30 (12H, m), 7.91 (2H, d, *J = 8.3 Hz*). MS^2 (ESI^+): m/z 536 ($M + H^+$), 269, 227, 167. Reaction of this methanesulfonate derivative (1 eq.) with 2eq. of EtONa in 2 mL MeOH at 50°C for 20h gave **20**, whereas a very similar reaction with 1 eq. of CH_3SNa in 1.5 mL dry DMF led to **21**. The reaction mixtures were extracted with CH_2Cl_2 and the products were purified by chromatography on SiO_2 (CH_2Cl_2 then 7 % MeOH).

h) Synthesis of 4-[4-(diphenylmethylene)piperidin-1-yl]-1-[4-tertiobutylphenyl]butan-1-one **22**, *1-[4-(2-aminoethyl)phenyl]-4-[4-(diphenymethylene)piperidin-1-yl]butan-1-one* **23**, *and 4-(diphenylmethylene)-1-[4-(4-tertiobutylphenyl)but-3-enyl]piperidine hydrochloride* **24**, *from dehydration of* **1**, **15** *and terfenadine, respectively.*

Derivative **1** (100 mg, 0.2 mmol) in 10 mL HCl (3 M, 30 mmol) was heated to reflux for 6h. After neutralization, the reaction mixture was extracted with CH_2Cl_2 and compound **22** was purified by TLC on SiO_2 (ethyl acetate, then 20 % EtOH).

Origins of recombinant cytochromes P450.

CYP2J2 was co-expressed with human P450 reductase in baculovirus-infected *Spodoptera frugiperda* insect cells (*Sf9*) and microsomes of these cells were prepared as described previously [11]. CYP2B6, 2C8, 2C9 and 3A4 were expressed in a previously described yeast strain W(R)fur1 [36] system, in which yeast cytochrome P450 reductase was overexpressed. Transformation by a pYeDP60 vector containing one of the human liver CYP2B6, 2C8, 2C9 and 3A4 cDNAs was then performed according to a general method of construction of yeast strain W(R)fur 1 expressing various human liver P450s [37-39]. Yeast culture and microsomes preparation were performed by using previously described techniques [40]. Microsomes were homogenized in 50 mM Tris buffer (pH 7.4) containing 1 mM EDTA and 20% glycerol (v/v), aliquoted, frozen under liquid N_2, and stored at -80 °C until use. P450 contents of yeast microsomes or insect cell microsomes were 90, 30, 30, 300 and 100 pmol P450/mg protein for CYP2B6, 2C8, 2C9, 3A4, and 2J2 respectively. Those contents were determined spectrally using the method of Omura and Sato [41]. Some comparative experiments were done using microsomes from baculovirus-infected insect cells expressing CYP 2B6, 2C8, 2C9, and 3A4 (Supersomes from BD Discovery Labware, Woburn, MA, USA).

Enzyme activity assays.

a) Hydroxylation of ebastine. The assay for hydroxylation of ebastine by CYP2J2 [24] was performed at 37 °C in the presence of a NADPH-generating system (1 mM $NADP^+$, 10 mM glucose 6-phosphate, and 2 units/mL glucose 6-phosphate dehydrogenase) using a previously described method [28]. The concentrations of ebastine and CYP2J2 were 0.5 µM and 1 nM, respectively. The reaction was done at 37 °C for 2 to 5 min.

b) O-Debenzylation of 7-benzyloxyresorufin. The protocol used for measuring the oxidation of 7-benzyloxyresorufin by CYP2B6 was based on a modification of the spectrofluorometric method described by Burke and Mayer [42]. A mixture containing 0.5 µM 7-benzyloxyresorufin and yeast microsomes expressing CYP2B6 (10 nM) in 100 mM HEPES buffer pH 7.8 containing 5 mM $MgCl_2$ for a total volume of 985 µL was preincubated at 37 °C for 3 min. Reaction was started with the addition of NADPH (100 µM) and formation of resorufin was monitored by fluorimetry, with an excitation wavelength of 535 nm and an emission wavelength at 580 nm. After 2 to 3 min, during this fluorimetric monitoring, inhibitor was added and the change of slope of the activity *vs.* time curve was observed. Then, quantitation of metabolite was done by addition of authentic resorufin (20 nM final concentration).

c) 6a-Hydroxylation of paclitaxel. Hydroxylation of paclitaxel by CYP2C8 [43] was assayed as described previously [44] (10 µM substrate, 10 nM CYP2C8, 5 min at 28 °C).

d) N-Deethylation of amodiaquine. N-deethylation of amodiaquine by microsomes of yeast cells expressing CYP2C8 was performed according to a previously reported procedure [45] (1 µM substrate, 10 nM CYP2C8, 10 min at 28 °C).

e) 4'-Hydroxylation of diclofenac. Diclofenac hydroxylation by CYP2C9 was carried out using a previously reported protocol [46] (15 µM substrate, 20 nM CYP2C9, 10 min at 28 °C).

f) 6β-Hydroxylation of testosterone. The assay for testosterone 6β-hydroxylation was performed as described previously [47] (20 µM substrate, 10 nM CYP3A4, 20 nM cytochrome b_5, 10 min at 28 °C).

Study of CYP2J2 inactivation by derivatives 5 and 13.

a) General incubation procedure. All incubations were performed at 37 °C in triplicate, using glass tubes in a shaking bath. The incubation mixture contained insect cell microsomes expressing CYP2J2, an inhibitor, and a NADPH-generating system in 0.1 M phosphate buffer pH 7.4 containing 1 mM EDTA.

*b) Time course analysis of the oxidation of compound **13** by CYP2J2-expressed insect cell microsomes.* Compound **13** was incubated at 37 °C in the presence of insect cell microsomes expressing CYP2J2 (10 nM) and reaction was started by the addition (t_0 = 0 min) of the NADPH-generating system, which had been pre-incubated at 37 °C for 3 min (total final volume of 2 mL). At t_0 and regularly thereafter, aliquots (200µL) were taken and were mixed with 100 µL of a cold CH_3CN/CH_3COOH (10:1) mixture to quickly stop the enzymatic reaction. Proteins were precipitated by centrifugation at 10 000 rpm for 10 min, and the supernatant was stored at –40°C for HPLC/MS/UV analysis. The apparatus for HPLC/MS-UV analysis was composed of a Surveyor HPLC system and LCQ Advantage-ion trap mass spectrometer (Thermo Finnigan, Les Ulis, France). Elution was carried out on a Betabasic-18 column (100 × 2.1 mm, 3.5 µ) (Thermo Finnigan, Les Ulis, France). The mobile phase consisted of water/acetonitrile/formic acid (80/20/1) (solvent A) and acetonitrile/formic acid (99/1) (solvent B), at a flow rate of 200 µL/min. Elution was performed with a linear gradient

from 0% to 45 % B in 5 min, followed by an increase of B to 55% in 17 min, and by 4 min at 100 % B. Quantification of the metabolite formed was carried by monitoring of the effluent at 310 and 275 nm.

c) Incubation for inactivation kinetics. The experimental protocols for determining the kinetic parameters of CYP2J2 inactivation were based on the previously described procedures for other mechanism-based inhibitors [48-50]. Insect cells microsomes (30 nM P450) were incubated under the conditions described above, in the presence of inhibitor concentrations ranging from 1 to 20 µM. At t_0 and regularly thereafter, aliquots (25 µL) were removed from the incubation medium and immediately processed to determine residual ebastine hydroxylase activity.

d) Determination of the residual monooxygenase activity. Routine experimental procedures to determine the enzymatic activity remaining after exposure to a suicide substrate [50] need the use of an alternative substrate to assay the remaining activity in a second incubation period. To dramatically decrease the influence of the already present inactivator substrate on the accurate determination of enzymatic activity, samples were diluted 20-fold in the standard medium assay. Briefly, 25 µL aliquots taken from CYP2J2 inactivation experiments were rapidly diluted in a total volume of 500 µL containing 20 µM ebastine and a NADPH-generating system. At t_0 = 0 min, 150 µL aliquots were removed and quenched by adding 75 µL of CH_3CN/CH_3COOH (10:1) cold mixture and vortexing. The remaining medium was incubated at 37°C and two other 150µL aliquots were removed at t = 2 and 4 min to be treated as the first one. In all experiments, the initial rate for ebastine hydroxylation activity was taken as a measure of the maximal activity (100 % activity).

e) Effect of a competitive inhibitor and glutathione on CYP2J2 inactivation by compound **13**. Incubations for inactivation measurement were carried out as described above

in order to determine the time course of enzyme inactivation in the presence of compound **4** or GSH. Compound **4** (50 μM) or GSH (5 mM) were added at t_0 of the inactivation incubation assay containing 5 μM compound **13**. At the indicated times, the residual activity was determined as described above. 100% activity was defined for remaining activity measured at t_0 for each incubation conditions. Control assays under non-catalysis conditions (in the absence of the NADPH-generating system) were carried out in parallel with the experimental incubations.

f) Inactivation kinetics analysis. Kinetic parameters of the inactivation process were calculated according to previously described models [48, 50]. This process can be represented in the simplest way by the following equations:

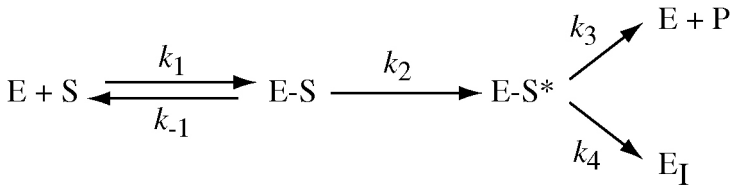

where ES is the initial enzyme-substrate complex converted to an activated species, ES*, that can either react with the enzyme which leads to inactivated enzyme (E_I), or break down to yield free enzyme and product (P). k_{-1}/k_1 represents the dissociation constant K_S, and k_3/k_4 is the partition ratio between the number of productive turnovers and the number of turnovers leading to enzyme inactivation. The pseudo-first order rate constant for the inactivation process (k_{inact}) is $k_2k_4/(k_2 + k_3 + k_4)$. The K_I constant, a term used for mechanism-based enzyme inactivators, is $[(k_{-1} + k_2)/k_1][(k_2 + k_4)/(k_2 + k_3 + k_4)]$. Calculation of those constants were performed using the analytical treatment described by Kitz and Wilson [51].

g) UV-visible spectra observed during interaction of compound **13** *with CYP2J2.* A suspension of microsomes from insect cells expressing CYP2J2 (100 nM P450) in 0.1 M phosphate buffer, pH 7.4, containing 0.1 mM EDTA was equally divided between two 200 μL black quartz cuvettes (1 cm path length). 3 μL of a DMSO solution of compound **13** were

added to the sample cuvette, the same volume of solvent being added to the reference cuvette, and a baseline was recorded between 350 and 500 nm. 2 µL of NADPH (final concentration of 100 µM) was then added (t_0 = 0 min) to the sample cuvette and difference spectra were recorded at t_0 and every min thereafter for 20 min between 350 and 500 nm.

RESULTS AND DISCUSSION

Synthesis of three series of derivatives of terfenadone, dehydroterfenadone and ebastine.

The choice of terfenadone, **1**, and ebastine as starting points for the design of high-affinity inhibitors of CYP2J2 was based on: (i) the high regioselectivity of the CYP2J2-catalyzed hydroxylations of **1** and ebastine, in favor of the least reactive part of these substrates (Fig.1), which implies their strict positioning in the CYP2J2 active site to keep their t-butyl group in close proximity of the heme iron for transfer of an oxygen atom from O_2, and (ii) the high affinity of **1** and ebastine for CYP2J2, as indicated by the IC_{50} value of **1** for CYP2J2 inhibition (0.7 µM) [28] and the *K*m of CYP2J2-catalyzed hydroxylation of ebastine (1 µM) [24].

Sixteen derivatives of terfenadone were synthesized and compared to terfenadone and the drug terfenadine, as CYP2J2 inhibitors (Table 1). Most of them derive from terfenadone by replacement of its t-butyl group with various **R** groups of different size and polarity. This includes **R** groups bearing chemical functions well known to lead to suicide inactivation of cytochrome P450 after *in situ* oxidation [52-56]. This is the case of the terminal double bond of compound **5**, of the CHF_2 function of compound **12**, and of the benzo-1,3-dioxole function of compound **13** (Table 1). The structure of compounds **5**, **12** and **13** was chosen so that the CYP2J2-catalyzed hydroxylation occurs at the site leading to inactivating metabolites, assuming that hydroxylation of these compounds should occur on the homobenzylic position, as the hydroxylation of terfenadone [28], terfenadine [27] and ebastine [24]. The general

synthetic route used for the preparation of the terfenadone and ebastine derivatives has been described previously [28]; it is recalled in Figure 2. Compounds **16** and **17**, in which the keto group of **1** and **4** was replaced with a CH_2 group, were also synthesized to evaluate the importance of this keto group in CYP2J2 inhibition. Compounds **5** and **14** were obtained from reaction of **11** with allytributyltin and imidazole, respectively. In the ebastine series, compounds **20** and **21** were prepared from reactions of the methanesulfonate of **19** with sodium ethanolate and sodium thiomethoxide, respectively (see Materials and Methods). Finally, compounds **22**, **23** and **24**, that are derived from dehydro-terfenadone, were obtained by treatment of compounds **1**, **15** and terfenadine by HCl in boiling water. All compounds were characterized by ^{1}H NMR spectroscopy and mass spectrometry. ^{1}H NMR spectroscopy in the presence of an internal standard showed that all these compounds were more than 95 % pure.

Comparison of the inhibitory effects of the terfenadone and ebastine derivatives towards CYP2J2.

The fourth columns of Tables 1, 2 and 3 compare the IC_{50} values found for the inhibition of ebastine hydroxylation catalyzed by recombinant CYP2J2 expressed in baculovirus-infected *Sf9* insect cells. These IC_{50} values vary from 0.4 to 23 µM.

The presence of a terminal hydrophobic group (Ph_2CHO-, $Ph_2C(OH)$- or Ph_2C=) in ω position relative to the hydroxylation site is important for the affinity of the inhibitors. This is indicated by the IC_{50} value of **25** that is 19-fold higher than that of terfenadone **1** (13 and 0.7 µM, respectively). The hydrophobicity of this terminal group appears to be the most important factor for the affinity, as the removal of the tertiary alcohol function of **1** or of the ether function of ebastine resulting in **22** does not lead to any significant loss of affinity (IC_{50} of 0.7 and 1 µM for **1** and ebastine to be compared to an IC_{50} of 0.9 µM for **22**).

The presence of the keto function *para* to the **R** group is also important for the affinity of the compounds. This is shown by the marked increase of the IC_{50} value observed after reduction of the CO function of **1** into CHOH or CH_2 functions (0.7, 8 and 3.6 µM for **1**, terfenadine and **16** respectively). Similar increases of IC_{50} by a factor of about 10 were also found when passing from **4** to **17** and from **22** to **24** (Tables 1 and 3).

The nature of the **R** substituent has a great influence on the affinity of the inhibitors towards CYP2J2. The best results were obtained with hydrophobic C_3 alkyl chains, as the lowest IC_{50} values were observed for compounds **4** and **5** (0.4 µM) for which **R** is a propyl or an allyl group. Any increase or decrease of the chain length, as in **6** or **3** respectively, led to an increase of the IC_{50} value. Moreover, the introduction of polar groups into **R** always led to a marked increase of the IC_{50} (compare for instance **7**, **8**, **9**, and **15** with **4** or **6**, and **10** with **3**). In that regard, the low IC_{50} value observed for compound **14**, for which **R** is a quite polar imidazole group, is a particular case. Its good affinity for CYP2J2 is due to the presence of the imidazole heterocycle, which is a well-known ligand of P450 iron [52] and should strongly bind to the iron of CYP2J2. Accordingly, addition of **14** to a suspension of microsomes from insect cells expressing CYP2J2 led, in difference visible spectroscopy, to a spectrum characterized by a peak at 432 nm and a trough at 415 nm (type II difference spectrum [57]) (data not shown). These data confirmed that **14** binds to CYP2J2 iron through the accessible nitrogen atom of its imidazole moiety.

Selectivity of the inhibitors towards CYP2J2 by comparison with other vascular P450s.

Tables 1-3 also compare the inhibitory effects of the terfenadone and ebastine derivatives towards the other main CYPs that have been reported to be present in the vascular vessels, namely CYP2B6, 2C8, 2C9 and 3A4 [58-61]. The reference activities that were followed to measure these inhibitory effects were 7-benzyloxyresorufin O-debenzylase [42], paclitaxel

6α-hydroxylase [43], diclofenac 4'-hydroxylase [62] and testosterone 6β-hydroxylase [47] respectively. The substrate concentrations used in these experiments were equal to the *K*m of the activity followed for each CYP (see Materials and Methods). Microsomes of the W(R)fur1 yeast strain expressing each CYP and overexpressing yeast cytochrome P450 reductase [36] were used. We have checked that the IC_{50} values measured with these systems were very similar to those measured by using microsomes of insect cells expressing CYP 2B6, 2C8, 2C9, and 3A4 in the case of compounds **1**, **3-6**, **11**, **13**, **14** and **17** (less than 15 % variation of the IC_{50} values).

Among all the studied compounds, the imidazole derivative **14** exhibited a particular behavior, as it acted as a good, but non selective inhibitor of all the studied CYPs, with IC_{50} values from 0.4 to 5.2 µM. However, it is noteworthy that it exhibited the best affinity for CYP2J2 (IC_{50} = 0.4 µM). Even though **14** is not a selective inhibitor for CYP2J2, it could be useful to inhibit all the vascular CYPs and, consequently, all the activities of arachidonic acid epoxidation at the vascular level.

As far as all the other compounds mentioned in Tables 1-3 are concerned, the main conclusions drawn from those tables are the following ones:

i) none of the studied compounds led to a significant inhibition of CYP2C8 (IC_{50} > 100 µM). In order to confirm these results, we have also studied the effects of the terfenadone and ebastine derivatives towards another usual CYP2C8 activity, the N-deethylation of amodiaquine [45]. Both CYP2C8-catalyzed activities were not significantly inhibited by compounds **1-25**, their IC_{50} values always being higher than 100 µM.

ii) CYP2C9 was inhibited with IC_{50} values between 10 and 69 µM, that were, in general, about 10 fold higher than those found for CYP2J2.

iii) the previous conclusion concerning CYP2C9 is globally valid for CYP2B6, with IC_{50} values varying from 7 to 90 µM, if one excludes compound **23** that appeared to be a very

good inhibitor of CYP2B6. This inhibitory effect of **23** towards CYP2B6, and to a lesser extent towards CYP2J2, could be due to a strong binding of its terminal NH_2 function to P450 iron.

iv) the studied compounds inhibited CYP3A4 with IC_{50} values from 0.9 to 68 µM, that were generally intermediate between those found for CYP2J2 and for CYP2C9 (or 2B6).

The best inhibitors of CYP2J2, **4** and **5**, are reasonably selective towards this cytochrome as their IC_{50} values towards the other studied CYPs are at least 20-fold (for **4**) and 14-fold (for **5**) higher than those found for CYP2J2.

This preliminary study of the IC_{50} values of the terfenadone and ebastine derivatives allowed us to select the following compounds for further, more detailed studies. Compound **4** was chosen because of its IC_{50} value of 0.4 µM that was the lowest one and of its good selectivity towards CYP2J2. The choice of compound **14** was made because of its low IC_{50} and because it could be considered as an inhibitor for all the main vascular CYPs. Finally, compounds **5** and **13** were selected because preliminary experiments showed us that their inhibitory effects increased as a function of the incubation time, suggesting that they could be mechanism-based inhibitors of CYP2J2.

Study of the mode of inhibition of CYP2J2 by 4.

Kinetic studies of the inhibition of CYP2J2-catalyzed hydroxylation of ebastine by **4** were performed at various ebastine (0.2 to 5 µM) and **4** (0 to 2 µM) concentrations. The Lineweaver-Burk plots of the reciprocal of the reaction rate *vs* the reciprocal of ebastine concentration, at different concentrations of **4**, indicated that **4** acts as a competitive inhibitor of CYP2J2 (intercept of the straight lines on the y axis [63], data not shown). The Dixon plot of 1/v *vs* the concentration of **4** led to a K_i value for the inhibition of CYP2J2 by **4** of 0.16 ± 0.05 µM (Figure 3). This value was in excellent agreement with the K_i value (0.2 µM) that

may be calculated from the IC_{50} value of Table 1, assuming that K_i=IC_{50}/2 for a competitive inhibitor [64].

Actually, **4** is a substrate of CYP2J2; it is hydroxylated at the level of its propyl group, as expected from its great analogy with terfenadone (P. Lafite *et al.*, publication in preparation). Thus, compound **4** is a competitive inhibitor and an alternative substrate of CYP2J2. We have checked that the concentration of **4** did not vary in a significant manner (less than 10 % consumption) under the conditions used in kinetic experiments of study of its inhibitory effects towards CYP2J2-catalyzed hydroxylation of ebastine (very low CYP2J2 concentration of 1 nM and short incubation times, 2-4 min).

Characterization of the inhibition of CYP2J2 by 14.

In order to analyze the type of inhibition of CYP2J2 by **14**, the Lineweaver-Burk plots of the reciprocal of the reaction rate *vs* the reciprocal of ebastine concentration were drawn at different **14** concentrations. Figure 4 shows that **14** acts as a mixed-type inhibitor of CYP2J2, with a competitive and a non-competitive component [65]. The Dixon plot drawn for the inhibition of CYP2J2-catalyzed hydroxylation of ebastine by **14** led to an evaluation of the competitive and the non-competitive inhibition constants K_i^C and K_i^{NC}, respectively (data not shown). The values deduced from the Dixon plot, K_i^C = 0.2 ± 0.1 µM and K_i^{NC} = 2.4 ± 0.4 µM, suggest that **14** is a mixed-type inhibitor, with a strong competitive component, as K_i^C is 10-fold higher than K_i^{NC}.

Mechanism of inhibition of CYP2J2 by compounds 5 and 13.

To further analyze the time-dependent variation of the inhibitory effects of **5** and **13**, insect microsomes containing recombinant CYP2J2 were preincubated with **5** or **13** in the presence or absence of NADPH (i.e. under catalysis or non catalysis conditions), and the remaining

enzymatic activity was measured using ebastine as substrate, as a function of the preincubation time.

Incubation of microsomes with **5** in the presence of NADPH led to a progressive loss of CYP2J2 activity as a function of time (Fig. 5A). With 20 µM **5**, 50 % of the activity was lost after 7 min and only 20 % remained after 20 min. Loss of CYP2J2 activity was faster after incubation with identical concentrations of **13**, as 50 % of the activity was lost after 1.5 min and only 20 % remained after 4 min in the presence of 20 µM **13** (Fig. 5B). Incubations under identical conditions but in the absence of NADPH did not lead to any significant loss of CYP2J2 activity. In the absence of either **5** or **13**, less than 10 % of the activity was lost after 10 min (data not shown). These results confirmed the existence of a catalysis-dependent inactivation of CYP2J2 upon oxidation of **5** and **13**.

Kinetics of CYP2J2 inactivation by **5** *and* **13**.

Figure 5A shows that the loss of CYP2J2 activity as a function of time after incubation in the presence of NADPH and various **5** concentrations followed the classical kinetics previously described for other CYP suicide-substrates [54, 55]. The time required for half-maximal inactivation, $t_{1/2}$, and the apparent first-order constant, k_{inact}, were calculated from the logarithmic transformation of the remaining activity as a function of time, as depicted in Figure 5A. Plots of $t_{1/2}$ versus reciprocal **5** concentration (Figure 5A, inset) led to the kinetic constants of the inactivation process (see Materials and Methods). From extrapolation to infinite **5** concentration, the time required to inactivate half of the enzyme, at the maximal rate, $t_{1/2max}$, and the maximal k_{inact} were 8.7 ± 2.2 min and 0.08 ± 0.02 min^{-1}, respectively (Table 4). The inhibition constant, K_I, was found to be 0.45 ± 0.05 µM, and the second-order rate constant k_{inact}/K_I, a proper index of the *in vitro* effectiveness of a compound as inactivator [66], was found to be 2960 ± 1000 $L.mol^{-1}.s^{-1}$.

Identical experiments were performed in the case of compound **13** (Figure 5B) and led to the kinetic constants reported in Table 4. The efficiencies of **5** and **13** as inactivators of CYP2J2 are similar, if one compares their k_{inact}/K_I values (2960 and 2700 $L.mol^{-1}.s^{-1}$, respectively). In fact, the inactivation rate of CYP2J2 by **13** is 6-times higher than that found in the case of **5** (0.47 ± 0.05 instead of 0.08 ± 0.02 min^{-1}). At the opposite, the affinity of **5** for CYP2J2 seems to be higher than that of **13**, as suggested by the K_I (0.45 ± 0.05 and 2.9 ± 0.2 µM respectively, Table 4) and IC_{50} values (0.4 ± 0.1 and 6.7 ± 2 µM, respectively, Table 1) found for these compounds. Table 4 also compares kinetic constants reported for other CYP mechanism-based inactivators [56]. It indicates that **5** and **13** are reasonably efficient mechanism-based inactivators of CYP2J2, as judged from their k_{inact}/K_I values.

Study of the molecular mechanism responsible for CYP2J2 inactivation by **13**.

Compound **13** has been designed to be a mechanism-based inhibitor of CYP2J2, as we expected that its hydroxylation by this enzyme would mainly occur at the level of its benzodioxole CH_2 group. Such P450-dependent oxidations of benzo-1,3-dioxole derivatives are well known to lead to the formation of the corresponding catechol metabolites and to P450 inactivation due to the formation of very stable P450 iron-benzodioxole-derived carbene complexes [52] (Figure 6). The generally admitted mechanism of these reactions involves the free-radical abstraction of an hydrogen atom of the benzodioxole CH_2 group by the high-valent P450 iron-oxo active species. The resulting radical may either undergo an oxidative transfer of the OH ligand of the P450 Fe(IV)-OH intermediate, with formation of an unstable orthoformiate that is eventually hydrolyzed to the corresponding catechol, or bind to P450 iron leading to a very stable P450 iron-carbene complex after elimination of H_2O [67, 68].

Addition of NADPH to microsomes of insect cells expressing CYP2J2 containing 100 µM **13** led to the progressive appearance of a difference visible spectrum characterized by two peaks at 428 and 457 nm (Figure 7). This difference spectrum is characteristic of the formation of a

P450 iron-benzodioxole-derived carbene complex [52]. Under the used conditions (0.1 µM CYP2J2, 100 µM **13**), the difference spectrum reached its maximal intensity 10 min after the addition of 100µM NADPH. If one considers the $\varepsilon_{455\text{-}490}$ nm values reported in the literature for the difference spectra of these P450 iron-carbene complexes, which vary from 50 000 to 75 000 $M.cm^{-1}$ [69, 70], one may estimate that 66 to 99 % of CYP2J2 is engaged in an iron-carbene complex derived from **13**.

Reaction mixtures from incubation of **13** with microsomes from insect cells expressing CYP2J2 in the presence of NADPH were studied by HPLC coupled to mass spectrometry. The major metabolite detected by this method exhibited a mass spectrum characterized by a molecular ion at m/z = 446 (M-12 if M is the molecular ion of **13**). This ion well corresponded to the one expected for the catechol derived from **13**. Moreover, the main fragments appearing in the mass spectrum of the metabolite were also in complete agreement with what could be expected for the catechol derived from **13**. Thus, most fragments exhibited m/z values equal to those of **13** minus 12, except the fragments that do not contain the benzodioxole moiety which exhibited m/z values identical to chose of the corresponding fragments of **13** (Figure 8). Finally, comparison of the UV spectra of **13** and of its main metabolite showed very similar characteristics with two peaks at 280 and 305-310 nm, and a small blueshift of the 305-310 nm peak for the metabolite of **13**. A comparison of the UV spectra of analog compounds, 3',4'-(methylenedioxy)-propiophenone and the corresponding catechol, led to very similar characteristics (data not shown).

The aforementioned data confirmed that CYP2J2-catalyzed oxidation of **13** mainly occurred at the benzodioxole CH_2 group with formation of the corresponding catechol metabolite and of a CYP2J2 iron-carbene complex that leads to the inactivation of this cytochrome.

Further studies of the characteristics of CYP2J2 inactivation by **13**.

Figure 9A shows that the loss of CYP2J2 activity upon incubation with 2 µM **13** for increasing times paralleled catechol metabolite formation, as expected for mechanism-based inhibition [48-50]. Figure 9B illustrates the correlation between the CYP2J2 activity remaining after oxidation of **13** and the amount of catechol metabolite formed for various concentrations of **13** and incubation times. The linear relationship observed allowed us to estimate the partition ratio of the inactivation process, *r*, which represents the number of productive turnovers (leading to the catechol metabolite) divided by the number of inactivating events [48-50]. Actually, extrapolation to 0 % remaining activity in Fig. 9B led to a *r* value of 18 ± 3.

The presence of **4**, a good competitive inhibitor and alternative substrate of CYP2J2, in incubations of CYP2J2 with **13** and NADPH led to a clear decrease of the rate of inactivation of CYP2J2 (see figure in Supplementary Materials).

An important property of efficient mechanism-based inhibitors is to generate reactive species that will rapidly react within the active site rather than diffuse out into solution. The presence of 5 mM reduced glutathione in incubations of CYP2J2 with **13** and NADPH did not have any significant effects on the rate of CYP2J2 inactivation (see figure in Supplementary Materials). This result indicates that the reactive intermediate of **13** that is responsible for CYP2J2 inactivation is not an electrophilic metabolite released in the medium. It is in agreement with the mechanism shown in Figure 6, in which the free radical intermediate from **13** is rapidly trapped by CYP2J2 iron, with the eventual formation of the iron-carbene complex, and is not released in the medium.

CONCLUSION

Starting from the structures of terfenadone and ebastine, 24 derivatives have been synthesized and evaluated as inhibitors of CYP2J2. Many of them exhibit a good affinity for this isoform

with IC_{50}s at the micromolar level. A comparison of these IC_{50}s has shown the importance of three structural features for a good recognition by CYP2J2: (i) the presence of a short hydrophobic alkyl chain at one end of the molecule, (ii) the presence of a keto group para to this alkyl chain on the terminal aryl group, and (iii) the presence of an hydrophobic diarylmethyl substituent at position 4 of the central piperidine ring. Four compounds appeared to be particularly interesting. Compound **14** is a good non-competitive (or mixed) inhibitor of CYP2J2 with an IC_{50} value of 400 ± 100 nM. It is not selective towards CYP2J2 as it also efficiently inhibits the other main vascular CYPs such as CYP2B6, 2C8, 2C9 and 3A4. However it could be an interesting tool to inhibit all these vascular CYPs. Compounds **4**, **5** and **13** are reasonably selective CYP2J2 inhibitors (Table 1). Compound **4** is a competitive inhibitor, alternative substrate of CYP2J2 of high-affinity (K_i = 160 ± 50 nM). Finally, compounds **5** and **13** are mechanism-based inhibitors of CYP2J2, characterized by high k_{inact}/K_I values (around 3000 $L.mol^{-1}.s^{-1}$) (Table 4). Inactivation of CYP2J2 by **13** is due to the formation of a very stable iron-carbene bond which occurs with a partition ratio of 18 ± 3.

Compounds **4**, **5** and **13** should be interesting tools to study the biological roles of CYP2J2. As far as vascular CYPs are concerned, Table 5 summarizes data obtained on **4** (this work, Table 1) and on ticlopidine [71, 72], montelukast [73], sulfaphenazole [74] and ketoconazole [74] as selective inhibitors of CYP2B6, 2C8, 2C9 and 3A4, respectively. These data show that each compound is a selective inhibitor of a given P450 – i.e. its IC_{50} for this CYP is at least 20-fold lower than its IC_{50} towards the other P450s –, and exhibits a high affinity for its preferred P450 (IC_{50} values between 20 nM for montelukast and ketoconazole towards CYP2C8 and 3A4 respectively, to 600 nM for sulfaphenazole towards CYP2C9). This set of compounds should be very useful to determine the biological role of each P450 in the cardiovascular system. Finally, given the recent findings suggesting that CYP2J2 may

represent a potential target for therapy of human cancers [23], studies are currently underway to test the above described CYP2J2 inhibitors as potential therapeutic agents for cancer.

ACKNOWLEDGEMENTS

We thank Dr. Didier Buisson (UMR8601) for a gift of compounds **2**, **10**, **16**, and **25**. This research was supported by the C.N.R.S. (Centre National de la Recherche Scientifique) and Ministère de la Recherche (France), and by the National Institutes of Environmental Health Sciences, National Institutes of Health (USA).

SUPPLEMENTARY MATERIALS

Supplementary data associated with this article (main ^{1}H-NMR and MS characteristics of compounds **1**, **3**, **4**, **6**, **9**, **11-13**, **15**, **17**, **5**, **14**, **7**, **8**, **19**, **18**, and **21-24**; Figure showing the effects of **4** or GSH on the rate of CYP 2J2 inactivation by **13**) can be found, in the online version of this article.

REFERENCES

[1] P.R. Ortiz de Montellano (Ed.), Cytochrome P450: Structure, Mechanism, and Biochemistry, Kluwer Academic/Plenum Publishers, New York, 2005.

[2] F.P. Guengerich, in: P.R. Ortiz de Montellano (Ed.), Cytochrome P450: Structure, Mechanism, and Biochemistry, Kluwer Academic/Plenum Publishers, New York, 2005, pp. 377-530.

[3] P.A. Williams, J. Cosme, A. Ward, H.C. Angove, D. Matak Vinkovic, H. Jhoti, Nature 424 (2003) 464-468.

[4] G.A. Schoch, J.K. Yano, M.R. Wester, K.J. Griffin, C.D. Stout, E.F. Johnson, J. Biol. Chem. 279 (2004) 9497-9503.

[5] M.R. Wester, J.K. Yano, G.A. Schoch, C. Yang, K.J. Griffin, C.D. Stout, E.F. Johnson, J. Biol. Chem. 279 (2004) 35630-35637.

[6] P.A. Williams, J. Cosme, D.M. Vinkovic, A. Ward, H.C. Angove, P.J. Day, C. Vonrhein, I.J. Tickle, H. Jhoti, Science 305 (2004) 683-686.

[7] J.K. Yano, M.R. Wester, G.A. Schoch, K.J. Griffin, C.D. Stout, E.F. Johnson, J. Biol. Chem. 279 (2004) 38091-38094.

[8] J.K. Yano, M.H. Hsu, K.J. Griffin, C.D. Stout, E.F. Johnson, Nat. Struct. Mol. Biol. 12 (2005) 822-823.

[9] P. Rowland, F.E. Blaney, M.G. Smyth, J.J. Jones, V.R. Leydon, A.K. Oxbrow, C.J. Lewis, M.M. Tennant, S. Modi, D.S. Eggleston, R.J. Chenery, A.M. Bridges, J. Biol. Chem. 281 (2005) 7614-7622.

[10] M. Ekroos, T. Sjogren, Proc. Natl. Acad. Sci. U.S.A. 103 (2006) 13682-13687.

[11] S. Wu, C.R. Moomaw, K.B. Tomer, J.R. Falck, D.C. Zeldin, J. Biol. Chem. 271 (1996) 3460-3468.

[12] P.E. Scarborough, J. Ma, W. Qu, D.C. Zeldin, Drug Metab. Rev. 31 (1999) 205-234.

[13] D.C. Zeldin, J. Foley, J. Ma, J.E. Boyle, J.M. Pascual, C.R. Moomaw, K.B. Tomer, C. Steenbergen, S. Wu, Mol. Pharmacol. 50 (1996) 1111-1117.

[14] D.C. Zeldin, J. Foley, S.M. Goldsworthy, M.E. Cook, J.E. Boyle, J. Ma, C.R. Moomaw, K.B. Tomer, C. Steenbergen, S. Wu, Mol. Pharmacol. 51 (1997) 931-943.

[15] A.A. Spector, X. Fang, G.D. Snyder, N.L. Weintraub, Prog. Lip. Res. 43 (2004) 55-90.

[16] I. Fleming, R. Busse, Hypertension 47 (2006) 629-633.

[17] J. Seubert, B. Yang, J.A. Bradbury, J. Graves, L.M. Degraff, S. Gabel, R. Gooch, J. Foley, J. Newman, L. Mao, H.A. Rockman, B.D. Hammock, E. Murphy, D.C. Zeldin, Circ. Res. 95 (2004) 506-514.

[18] M. Spiecker, H. Darius, T. Hankeln, M. Soufi, A.M. Sattler, J.R. Schaefer, K. Node, J. Borgel, A. Mugge, K. Lindpaintner, A. Huesing, B. Maisch, D.C. Zeldin, J.K. Liao, Circulation 110 (2004) 2132-2136.

[19] Y.F. Xiao, Q. Ke, J.M. Seubert, J.A. Bradbury, J. Graves, L.M. Degraff, J.R. Falck, K. Krausz, H.V. Gelboin, J.P. Morgan, D.C. Zeldin, Mol. Pharmacol. 66 (2004) 1607-1616.

[20] T. Lu, D. Ye, X. Wang, J.M. Seubert, J.P. Graves, J.A. Bradbury, D.C. Zeldin, H.C. Lee, J. Physiol. 575 (2006) 627-644.

[21] Y. Wang, X. Wei, X. Xiao, R. Hui, J.W. Card, M.A. Carey, D.W. Wang, D.C. Zeldin, J. Pharmacol. Exp. Ther. 314 (2005) 522-532.

[22] U.R. Michaelis, I. Fleming, Pharmacol. Ther. 111 (2006) 584-595.

[23] J.G. Jiang, C.L. Chen, J.W. Card, S. Yang, J.X. Chen, X.N. Fu, Y.G. Ning, X. Xiao, D.C. Zeldin, D.W. Wang, Cancer Res. 65 (2005) 4707-4715.

[24] T. Hashizume, S. Imaoka, M. Mise, Y. Terauchi, T. Fujii, H. Miyazaki, T. Kamataki, Y. Funae, J. Pharmacol. Exp. Ther. 300 (2002) 298-304.

[25] K.H. Liu, M.G. Kim, D.J. Lee, Y.J. Yoon, M.J. Kim, J.H. Shon, C.S. Choi, Y.K. Choi, Z. Desta, J.G. Shin, Drug Metab. Dispos. 34 (2006) 1793-1797.

[26] S. Matsumoto, T. Hirama, T. Matsubara, K. Nagata, Y. Yamazoe, Drug Metab. Dispos. 30 (2002) 1240-1245.

[27] S. Parikh, P. Gagne, V. Miller, C. Crespi, K. Thummel, C. Patten, Drug Metab. Rev. 35 (2003) 190-190.

[28] P. Lafite, S. Dijols, D. Buisson, A.C. Macherey, D.C. Zeldin, P.M. Dansette, D. Mansuy, Bioorg. Med. Chem. Lett. 16 (2006) 2777-2780.

[29] A.A. Carr, C.R. Kinsolving, U.S. Patent 3,862,173 (1975).

[30] M.Q. Zhang, Y. Wada, F. Sato, H. Timmerman, J. Med. Chem. 38 (1995) 2472-2477.

[31] R. Bujok, M. Makosza, Synlett (2002) 1285-1286.

[32] J.V. Bhashkar, M. Periasamy, J. Org. Chem. 56 (1991) 5964-5965.

[33] Y. Kawakami, H. Kitani, S. Yuasa, M. Abe, M. Moriwaki, M. Kagoshima, M. Terasawa, T. Tahara, Eur. J. Med. Chem. 31 (1996) 683-692.

[34] B. Di Giacomo, D. Coletta, B. Natalini, M.H. Ni, R. Pellicciari, Il Farmaco 54 (1999) 600-610.

[35] H. Zhang, Q. Cai, D. Ma, J. Org. Chem. 70 (2005) 5164-5173.

[36] G. Truan, C. Cullin, P. Reisdorf, P. Urban, D. Pompon, Gene 125 (1993) 49-55.

[37] A. Bellamine, J.C. Gautier, P. Urban, D. Pompon, Eur. J. Biochem. 225 (1994) 1005-1013.

[38] L. Gervot, B. Rochat, J.C. Gautier, F. Bohnenstengel, H. Kroemer, V. de Berardinis, H. Martin, P. Beaune, I. de Waziers, Pharmacogenetics 9 (1999) 295-306.

[39] J.P. Renaud, C. Cullin, D. Pompon, P. Beaune, D. Mansuy, Eur. J. Biochem. 194 (1990) 889-896.

[40] D. Pompon, B. Louerat, A. Bronine, P. Urban, Methods Enzymol. 272 (1996) 51-64.

[41] T. Omura, R. Sato, J. Biol. Chem. 239 (1964) 2370-2378.

[42] M.D. Burke, R.T. Mayer, Chem. Biol. Interact. 45 (1983) 243-258.

[43] A. Rahman, K.R. Korzekwa, J. Grogan, F.J. Gonzalez, J.W. Harris, Cancer Res. 54 (1994) 5543-5546.

[44] A. Melet, C. Marques-Soares, G.A. Schoch, A.C. Macherey, M. Jaouen, P.M. Dansette, M.A. Sari, E.F. Johnson, D. Mansuy, Biochemistry 43 (2004) 15379-15392.

[45] X.Q. Li, A. Bjorkman, T.B. Andersson, M. Ridderstrom, C.M. Masimirembwa, J. Pharmacol. Exp. Ther. 300 (2002) 399-407.

[46] A. Melet, N. Assrir, P. Jean, M. Pilar Lopez-Garcia, C. Marques-Soares, M. Jaouen, P.M. Dansette, M.A. Sari, D. Mansuy, Arch. Biochem. Biophys. 409 (2003) 80-91.

[47] W.R. Brian, M.A. Sari, M. Iwasaki, T. Shimada, L.S. Kaminsky, F.P. Guengerich, Biochemistry 29 (1990) 11280-11292.

[48] C. Walsh, Tetrahedron 38 (1982) 871-909.

[49] M.P. Lopez-Garcia, P.M. Dansette, D. Mansuy, Biochemistry 33 (1994) 166-175.

[50] R.B. Silverman, in: D.L. Purich (Ed.), Enzyme Kinetics and Mechanism Part D: Developments in Enzyme Dynamics, Academic Press, 1995, pp. 240-283.

[51] R. Kitz, I.B. Wilson, J. Biol. Chem. 237 (1962) 3245-3249.

[52] M.A. Correira, P.R. Ortiz de Montellano, in: P.R. Ortiz de Montellano (Ed.), Cytochrome P450: Structure, Mechanism, and Biochemistry, Kluwer Academic/Plenum Publishers, New York, 2005, pp. 247-322.

[53] B. Testa, P. Jenner, Drug Metab Rev 12 (1981) 1-117.

[54] J.R. Halpert, J.C. Stevens, Methods in enzymology 206 (1991) 540-548.

[55] U.M. Kent, M.I. Juschyshyn, P.F. Hollenberg, Curr. Drug Metab. 2 (2001) 215-243.

[56] E. Fontana, P.M. Dansette, S.M. Poli, Curr. Drug. Metab. 6 (2005) 413-454.

[57] C.R. Jefcoate, Methods in enzymology 52 (1979) 258-279.

[58] B.G. Hoebel, E. Steyrer, W.F. Graier, Clin. Exp. Pharmacol. Physiol. 25 (1998) 826-830.

[59] B. Fisslthaler, R. Popp, L. Kiss, M. Potente, D.R. Harder, I. Fleming, R. Busse, Nature 401 (1999) 493-497.

[60] J. Borlak, M. Walles, K. Levsen, T. Thum, Drug Metab. Dispos. 31 (2003) 888-891.

[61] T.C. DeLozier, G.E. Kissling, S.J. Coulter, D. Dai, J.F. Foley, J.A. Bradbury, E. Murphy, C. Steenbergen, D.C. Zeldin, J.A. Goldstein, Drug Metab. Dispos. In press (2007).

[62] A. Mancy, M. Antignac, C. Minoletti, S. Dijols, V. Mouries, N.T. Duong, P. Battioni, P.M. Dansette, D. Mansuy, Biochemistry 38 (1999) 14264-14270.

[63] M. Dixon, E.C. Webb, Enzymes, Academic Press Inc., New York, 1964.

[64] Y. Cheng, W.H. Prusoff, Biochem. Pharmacol. 22 (1973) 3099-3108.

[65] I.H. Segel, Enzyme kinetics, Wiley-Interscience, New York, 1993.

[66] P.J. Bednarski, S.D. Nelson, J. Med. Chem. 32 (1989) 203-213.

[67] D. Mansuy, J.P. Battioni, J.C. Chottard, V. Ullrich, J. Am. Chem. Soc. 101 (1979) 3971-3973.

[68] D. Mansuy, P. Battioni, J.P. Battioni, Eur. J. Biochem. 184 (1989) 267-285.

[69] C.R. Elcombe, J.W. Bridges, T.J.B. Gray, R.H. Nimmo-Smith, K.J. Netter, Biochem. Pharmacol. 24 (1975) 1427-1433.

[70] M. Murray, C.F. Wilkinson, C. Marcus, C.E. Dube, Mol. Pharmacol. 24 (1983) 129-136.

[71] N.T. Ha-Duong, S. Dijols, A.C. Macherey, J.A. Goldstein, P.M. Dansette, D. Mansuy, Biochemistry 40 (2001) 12112-12122.

[72] T. Richter, T.E. Murdter, G. Heinkele, J. Pleiss, S. Tatzel, M. Schwab, M. Eichelbaum, U.M. Zanger, J. Pharmacol. Exp. Ther. 308 (2004) 189-197.

[73] R.L. Walsky, R.S. Obach, E.A. Gaman, J.P. Gleeson, W.R. Proctor, Drug Metab. Dispos. 33 (2005) 413-418.

[74] S.J. Baldwin, J.C. Bloomer, G.J. Smith, A.D. Ayrton, S.E. Clarke, R.J. Chenery, Xenobiotica 25 (1995) 261-270.

[75] K.M. Bertelsen, K. Venkatakrishnan, L.L. Von Moltke, R.S. Obach, D.J. Greenblatt, Drug Metab. Dispos. 31 (2003) 289-293.

[76] P.J. Ciaccio, D.B. Duignan, J.R. Halpert, Drug Metab. Dispos. 15 (1987) 852-856.

[77] E.S. Roberts, N.E. Hopkins, W.L. Alworth, P.F. Hollenberg, Chem. Res. Toxicol. 6 (1993) 470-479.

LEGENDS OF FIGURES

Figure 1: Regioselectivity of the hydroxylation of ebastine and terfenadone by CYP2J2.

Figure 2: General synthetic routes used for the preparation of terfenadone and ebastine derivatives. For the nature of **R**, see Table 1 and 2. Specific protection and deprotection of reactive chemical functions were used when necessary. They were mentioned in ref [28].

Figure 3: Dixon plots obtained from a kinetic study of CYP2J2-catalyzed hydroxylation of ebastine in the presence of different concentrations of compound 4. Results are means ± SD calculated from three independent experiments, using microsomes of insect cells expressing CYP2J2, ebastine, **4**, and a NADPH generating system, as described in Materials and Methods. Substrate concentrations used were 0.2 (■), 0.5 (Δ), 2 (▲) and 5 µM (○).

Figure 4: Lineweaver-Burk plots obtained from a kinetic study of CYP2J2-catalyzed hydroxylation of ebastine in the presence of different concentrations of compound 14. Results are means ± SD calculated from three independent experiments, using microsomes of insect cells expressing CYP2J2, ebastine, **14** and a NADPH generating system. Inhibitor concentrations used were 0 (□),0.5 (▲), 1 (○) and 2.5 µM (●).

Figure 5: Kinetics of inactivation of CYP2J2 upon NADPH-dependent oxidation of compounds 5 (A) and 13 (B). Details for incubations and determination of remaining activity are described in Materials and Methods. CYP2J2 (30 nM) was incubated for the indicated times in the presence of a NADPH-generating system and 0 (■), 1 (□), 2 (▲), 5 (Δ) and 20 µM (○) compound **5** or **13**. Values are means calculated from three independent experiments.

The inset shows the plot of $t_{1/2}$ (time required for half-inactivation of CYP2J2) *vs* the reciprocal of the concentration of **5** or **13** for the experiments depicted (Kitz-Wilson plot).

Figure 6: Possible mechanisms of the CYP2J2-catalyzed oxidation of 13 and of the inactivation of this cytochrome.

Figure 7: Difference absorption spectra observed during CYP2J2-catalyzed oxidation of 13 in the presence of NADPH. Conditions described in Materials and Methods; difference spectra obtained after 2,5, and 10 min after addition of 100 µM NADPH to the sample cuvette containing 0.1 µM CYP2J2 and 100 µM **13**.

Figure 8: Mass spectra of compound 13 and its metabolite formed after oxidation by CYP2J2. Mass spectra were obtained from HPLC-MS^2 analysis of incubations of 50 µM **13** with 10 nM CYP2J2 and a NADPH-generating system for 20 min, as described in Materials and Methods. The molecular fragments corresponding to the observed peaks are shown. (-H_2O: 250) indicates the fragment having lost H_2O from dehydration of the tertiary alcohol function.

Figure 9: Relationship between CYP2J2 inactivation and efficient catalysis of 13 oxidation (catechol metabolite formation) (A) and determination of the partition ratio (B). Microsomes from insect cells expressing CYP2J2 were incubated with 2 µM **13** and a NADPH generating system (A). Values are means ± SD calculated from 3 independent experiments. Curve (B) was obtained from residual CYP2J2 activities and amounts of catechol metabolites measured from incubations of microsomes containing CYP2J2 in the

presence of a NADPH generating system and various concentrations of **13** (2-20 μM) for different time periods (0 to 30 min). Points are mean values from 3 experiments.

Figure 1

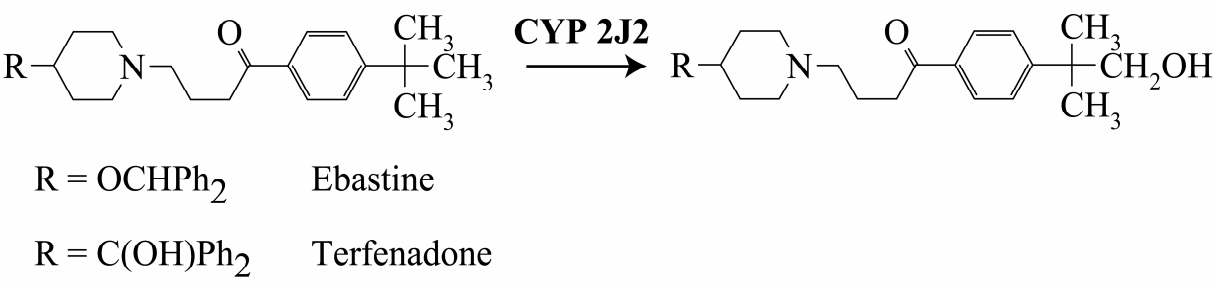
R
N
O
CH3
CH3
CH3
CYP 2J2
R
N
O
CH3
CH2OH
CH3
R = OCHPh2 Ebastine
R = C(OH)Ph2 Terfenadone

Figure 2

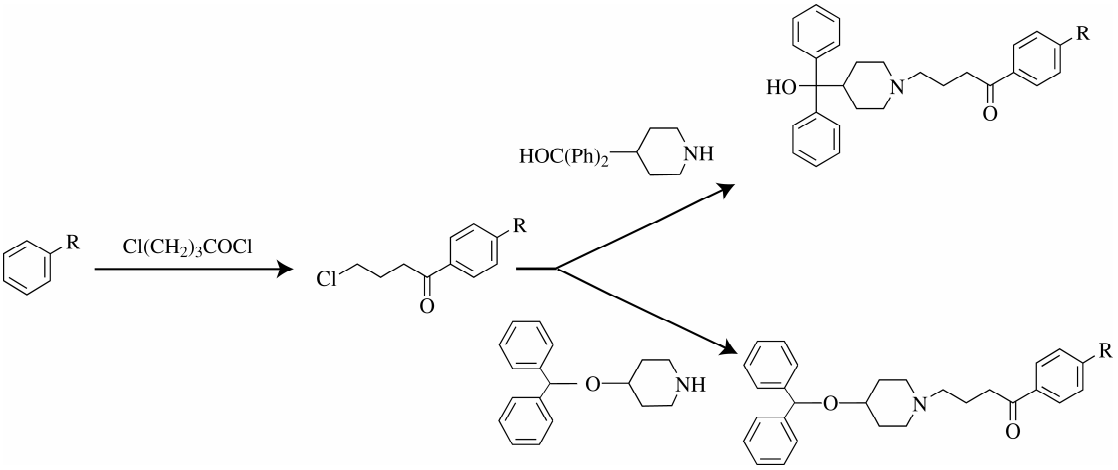

Figure 3

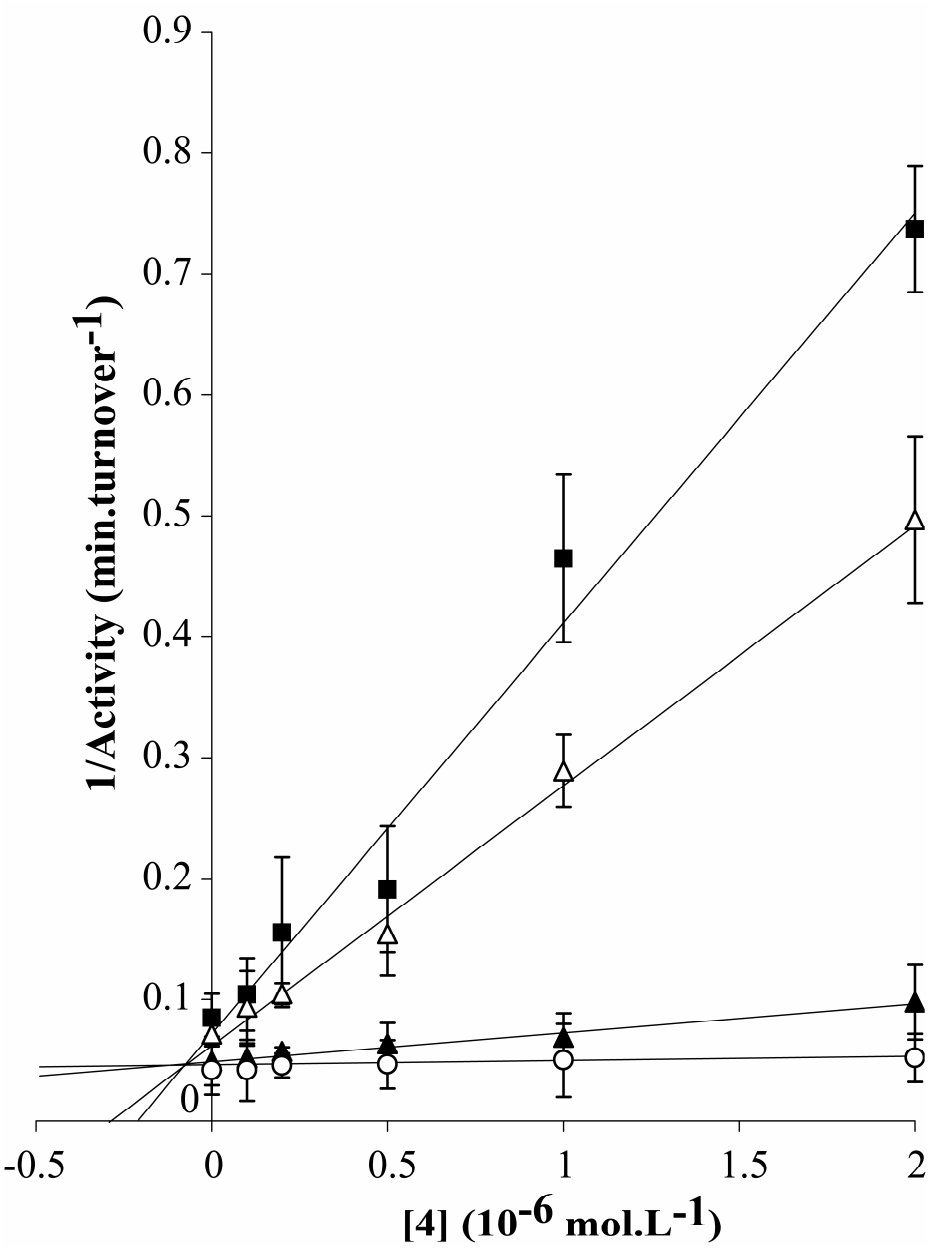
0.9
0.8
0.7
0.6
0.5
0.4
0.3
0.2
0.1
0
1/Activity (min.turnover-1)
-0.5
0
0.5
1
1.5
2
[4] (10-6 mol.L-1)